Ninth Canadian Conference on
Earthquake Engineering
Ottawa, Ontario, Canada
26-29 June 2007

NETWORKED HYBRID TESTS OF A 4-PIER DOUBLE-SKINNED CFT BRIDGE

M.-L. Lin[1], Y.-T. Weng[1], Y.-S. Yang[1], S.-J. Wang[1],
P.-C. Chen[1], K.-C. Tsai[2], D. Lau[3], Y.-Y. Chang[4] and H. A. Khoo[5]

ABSTRACT

Pseudo-dynamic tests (PDTs) on a reduced-scale model of a four-pier bridge were performed at the National Center for Research on Earthquake Engineering (NCREE) and at the National Taiwan University (NTU), which are both in Taiwan, and at Carleton University (CU) in Canada. These tests were performed using the sub-structuring technique and were completed in February, 2006. Three physical pier specimens were constructed and tested in these three laboratories, while the deck, the abutments and the remaining one pier were numerically modeled on-line. The seismic ground accelerations considered in this study were either based on the recorded data of the 1999 Chi-Chi earthquake or were generated for site conditions in Western Canada. The ground accelerations were scaled up to the representative return periods of 50%, 10%, and 2% in 50 years and bi-directionally applied in the transverse and longitudinal directions simultaneously. This study is aimed at the assessment of the seismic vulnerability of a typical high-speed railway bridge system designed prior to the modern Taiwan bridge seismic code. The seismic performance of the prototype bridge structure was predicted by nonlinear structural analysis programs, namely, PISA3D and OpenSEES. DSCFT bridge pier system performed extremely well after the application of four earthquake loads. Test results confirmed that the earthquake responses of the DSCFT bridge piers system can be predicted satisfactorily using both PISA3D and OpenSEES.

Introduction

The concept of an Internet-based, multiple-site network and hybrid testing of structural systems has been developed to overcome the facility limitation problem of an individual laboratory. This was accomplished by subdividing a single test experiment into sub-components to be tested or simulated simultaneously at multiple laboratories linked through the network in real time. Similar concepts of this Internet-based virtual laboratory testing at multiple sites are currently being developed and implemented by researchers in many countries, such as the NEES Project (Rietherman 2004) in the United States, ED-Net (Ohtani et al. 2002) in Japan, KOCED (Kim 2004) in Korea, and ISEE (Yang et al. 2003, Wang et al. 2003) in Taiwan. These sites all aim to revolutionize earthquake engineering research by providing researchers at different laboratories anywhere around the world the means to collaborate and to conduct networked collaborative hybrid experiments.

[1]Associate Research Fellow, National Center for Research on Earthquake Engineering, Taipei, Taiwan
[2]Director, National Center for Research on Earthquake Engineering, Taipei, Taiwan
[3]Professor, Department of Civil and Environmental Engineering, Carleton University, Ottawa, Canada
[4]PhD Candidate, Department of Civil and Environmental Engineering, Carleton University, Ottawa, Canada
[5]Research Assistant, Department of Civil and Environmental Engineering, Carleton University, Ottawa, Canada

A joint collaboration among three engineering laboratories; the National Center for Research on Earthquake Engineering (NCREE); the National Taiwan University (NTU), which are both in Taiwan, and Carleton University (CU) in Canada; was established to perform a transnational collaborative pseudo-dynamic experiment to simulate the response of a multi-span bridge system (see Fig. 1) subjected to a series of bi-lateral ground motions. Three of the testing pier specimens were located at Carleton University (CU), NCREE, and NTU. The fourth pier, P4, and the superstructure were simulated numerically by finite element models. A platform named Internet-based Simulation for Earthquake Engineering (ISEE) was employed for the data repository and communication among the laboratories. The main objectives of this collaborative experiment are: to evaluate the performance of the ISEE network hybrid testing environment; to study the dynamic behavior of the double-skinned concrete filled tubular (DSCFT) columns; to evaluate the efficiency of the column-foundation connection under bi-lateral excitations; and to evaluate the methods and techniques developed for numerical analyses.

The test specimens were designed to comply with the similitude requirements following Buckingham's theorem (Harris and Sabnis, 1999) for a direct reduced-scale model of the prototype bridge as shown in Fig. 1. Different scaling factors were used in the design of the sub-component test specimens at the multiple test sites, based on the available testing equipment and physical size of each of the participating laboratory sites. In addition, the scale factors for displacement were chosen to be 1/5 for the Carleton University and NTU laboratories and 2/5 for the NCREE Laboratory. The test specimens were loaded pseudo-dynamically using input ground motions from the 1999 Chi-Chi earthquake and the simulated Cascadia earthquake in Vancouver, Canada, and were scaled to representative seismic hazard levels of 50%, 10%, and 2% probability of exceedance in 50 years.

Collaborative Experiments Using Hybrid Reduced-Scale Specimens

This transnational pseudo-dynamic experiment scales down the experimental specimens according to the practical situation of each laboratory, including the laboratory space limitations, reaction wall or support sizes, actuator forces, and strong floor forces. The scaled pier heights at CU, NCREE, and NTU laboratories are 2m, 6m and 3m respectively. It should be noted that the total specimen heights are higher than the pier height. Extra height includes the foundations, actuator connection, and pre-stressed cables for the axial force. The required laboratory space is commonly much larger than the specimen's size. For example, the specimen height at NCREE is 8.32m, and it requires up to 16.6m of clear height space during specimen assemblage and installation. The detailed experimental setup is introduced in (Yang et al., 2005).

Design of Bridge Systems and Specimen

Description of prototype bridge structure

The typical prototype bridge structure is illustrated in Fig. 1. The structure was assumed to be designed for a highly seismic location in either Taiwan or Western Canada. All bridges have four 40 m spans, and a typical deck width of 9.75 m has been found to be in common in Taiwan and Canadian bridge configurations. Three DSCFT pier heights of 10, 12 and 15 m (which are typically found in most highway bridges) were used as an asymmetrical bridge system, and the piers were assumed to be fully fixed at the base and pinned at its connection to the superstructure. The bridge system considered in this study was assumed to have a hat beam above each DSCFT column, and each hat beam was connected rigidly to the steel girder using a simple connection that provides a free rotation of the support. The bridge deck was taken to be a 230mm thick reinforced concrete slab built composite with steel girder spaced at 2.6m. The slab was designed to have a 1m overhang on both sides of the deck. The pavement was adopted to be 80mm thick. The weight of the superstructure including deck and steel girder was presumed as 19.5 tonf/m, and the weight of DSCFT columns P1, P2, P3, P4 were 13.2, 19.2, 13.2, and 19.2 tonf/m, respectively. The depth of cap beams range among 1.5, 2.5, and 3.0m. Fig. 2 shows the dimensions of the superstructure of the prototype bridge. This prototype bridge was designed according to the Taiwan's

bridge seismic provision (DOT, 1995). The bridge structure was assumed to be located in Chiayi City or Vancouver with Soil Type I (hard rock site), and with an occupancy importance factor I of 1.0. All steels used were A36 type with a yielding strength of 250 MPa. The design load combination adopted was 1.0DL+1.0EQ. It should be noted that the design spectra with spectral accelerations for the 10/50 event (Fig. 3a) are normalized spectral acceleration factor C = 1.25, seismic zone factor Z = 0.33, and seismic force reduction factor Fu = 2.0, while for the 2/50 event (Fig. 3b), according to the NBCC 2005 draft (NBC, 2004), the specific spectral accelerations in Vancouver City were referred from the list in Table 1. Finally, the seismic lateral design base shear V = 0.173W represents the stage of significant yielding of the system for the 10/50 event.

Table 2 and Table 3 list the sectional properties, stiffness and yielding strength of the four bridge piers and the superstructure. Full composite action between the slab and the steel girder was assumed in the calculation of the superstructure's stiffness. The lateral stiffness of each column was calculated assuming cantilever behavior, since pinned and fixed connections were provided at the upper and lower ends of each column respectively. For DSCFT columns, the theoretical flexural stiffness adopted for this study follows the definition given for CFT (Hsu and Lin, 1997; Zhong, 1999):

$$EI=(0.6625+0.9375\alpha)(E_S I_S+\beta E_C I_C) \quad (1)$$

where $\alpha = A_S/A_C$. The elastic modulus of the concrete was estimated from $E_C = 4730\sqrt{f'_C}$ (MPa), and the elastic modulus for the steel tube, E_S, was set as 2×10^5 MPa, I_S and I_C are the moment of inertia of steel and concrete respectively. According to the experimental results, β is approximately 0.12 (Lin et al. 2001). Compressive strength calculations for concrete-filled steel columns are the same as for bare steel structural members in AISC (1994) with the exception that modified properties F_{my}, E_m and r_m are used. The axial design strength, P_n was calculated as:

$$P_n = A_S F_{cr} \quad (2)$$

$$F_{cr} = \left(0.658^{\lambda_C^2}\right)F_{my} \quad for\ \lambda_C \le 1.5 \quad (3a)$$

$$F_{my} = f_y + 0.85 f'_C\left(A_C / A_S\right) \quad (3b)$$

$$\lambda_C^2 = \left(KL/\pi r_m\right)^2\left(F_{my}/E_m\right) \quad (3c)$$

$$E_m = E_S + 0.4 E_C A_C / A_S \quad (3d)$$

where KL = effective length of simply supported column and r_m = radius of gyration of steel tube.

This prototype bridge system was assumed to have sliding or pot bearings. Pot bearings are generally used in medium-span modern steel bridges (Barker and Puckett, 1997; Demetrios, 1995). Sliding bearings were used commonly in the past for short-span steel bridges (Demetrios 1995). Both types of bearings are normally pin-connected in the transverse and longitudinal directions. In the longitudinal direction, both ends of the bridge are generally expansion bearings (rollers). Based on the seismic design procedures mentioned above, the axial load of the piers was found and is listed in Table 5. The force requirements of each pier are listed in Table 4. According to the axial load and moment requirements, the diameter and thickness of the DSCFT columns were designed and are shown in Table 4. Axial stress in the columns of less than 10% sectional axial load capacity was the adopted criteria to design the column sections. The embedded DSCFT-to-foundation connection (Wei, 2002) was used to design the connections of the DSCFT columns. Table 5 shows the details of scaling-down the specimens for testing.

Test Setup

Two hydraulic MTS actuators were used for the P2 specimen in the longitudinal (noted as X-direction) and transverse (noted as Y-direction) direction. Similarly, one hydraulic MTS actuator was used for P1 and P3 specimens in the X and Y directions, respectively. Vertical loads of about 409 kN, 2174 kN, and 609 kN were applied to axially compress the P1, P2, and P3 specimens, respectively. The foundation was

attached to the laboratory's strong floor using several high-strength bolts. A horizontal loading beam was used to transfer the vertical axial load to the column. Fig. 4 shows the final test setup of the P1, P2, and P3 specimens.

Bi-Directional Ground Motions and Experimental Scenario

According to IBC2000 provisions (ICC, 2000) and the recommendations of the Sa(T1) method provided by Shome et al. (1998), for each pair of (bi-lateral) horizontal ground motion components, the square root of the sum of the square (SRSS) of the 5% damped site-specific spectra of the scaled horizontal components shall be constructed. The ground motions shall be scaled such that the spectral acceleration of the SRSS spectra is not less than 1.4 times the 5% damped smoothed design spectra at the fundamental period of the prototype building in the considered direction. In addition, the scaling factor (denoted as SF) should not exceed a value of 4.0. The original CHY024 and M65R40T4 acceleration time-histories are shown in Fig. 5. The corresponding spectra representing 10/50 and 2/50 hazard levels that satisfied the above mentioned requirements are shown in Fig. 3. The earthquake scenario, including the earthquake intensities and sequence, for this experiment is shown in Fig. 6. Fig. 7 also shows the three earthquake ground accelerations used in the longitudinal and transverse directions, which are 50/50 (M65R40T4), 10/50 (CHY024), and 2/50 (M65R40T4), respectively.

This experiment simulated bi-lateral seismic responses of the multi-span bridge induced by a series of bi-directional ground motions. The corresponding spectral curves representing 10/50 levels of Taiwan 1995 bridge seismic provision and satisfying the above-mentioned requirements of the Sa (T1) method are shown in Fig. 3a. Similarly, the corresponding spectral curves, representing 2/50 levels of NBC 2005 draft (NBC, 2005) and satisfying the above-mentioned requirements of the Sa (T1) method, are shown in Fig. 3b.

Modeling for Analysis

Inelastic static and dynamic time history analyses were conducted using PISA3D (Tsai and Lin, 2003) and OpenSEES (Open System for Earthquake Engineering Simulation) (McKenna and Fenves 2000), which utilizes force–displacement hysteretic rules to characterize non-linear response. These systems were developed at the National Taiwan University and the Pacific Earthquake Engineering Research Center (PEER), respectively. The simplified structural model is presented in Fig. 8. The superstructure was modeled as a beam-column element. Each span was divided into 4 segments and the superstructure mass was lumped at each nodal point connecting the beams. The location of each lumped mass point was elevated to the level of the center of gravity of the bridge deck using a vertical rigid link element attached to it. Each beam cap of the bridge pier was modeled also as a rigid link element connected to the bridge pier. Figure 9 shows the simplified structural model and the prototype specimen of each DSCFT bridge pier.

PISA3D Model

In the application of PISA3D, considering the degrading-strength behavior of the concrete, all DSCFT columns were modeled using the three-parameter degrading beam-column elements (Tsai and Lin 2003a). It was evident that the hysteretic behavior of CFT column members simulated by PISA3D shown in Fig. 10 was satisfactory and agreed well with the results of the experiments obtained from the DSCFT column specimen S24 cyclic load test (Tsai et al., 2004). All the upper structural members were modeled using the bi-linear beam-column elements (Fig. 11). All analytical processes have considered the second-order effects.

OpenSEES Model

The displacement-based beam-column element using fiber sections, FEDEAS (Filippou 1996) steel model (steel02) and concrete model (concrete02) were used in the numerical simulation.

Nonlinear Analysis and Seismic Demand Prediction

In order to estimate the deformational demand in terms of meeting the earthquake hazard levels, and

equipment demand of this pseudo dynamic test, the bridges were subjected to dynamic inelastic time-history analysis. However, a certain amount of scatter in the time histories and their associated design response spectra was expected. The researchers would have expected a proportional amount of scatter in the results of analysis as well. For this prototype bridge designed according to the design earthquake spectra, the corresponding earthquake scenario calculated by the Sa (T1) method was employed in the analysis.

After extensive nonlinear time-history analyses, the earthquake scenario including the earthquake intensities and sequence for this experiment shown in Fig. 6, enabled the demands on test equipment (actuators, instrumentation) be estimated accurately to insure the adequacy of the used equipment. Analytical results represented an envelope of maximum responses. Fig. 12 shows peak bridge column base shear for the 2/50 level of excitation. The peak column base shear predicted by the NLRHA in X direction were about 6812 kN, 5000 kN, and 9112 kN (3590 kN , 5568 kN, and 5501 kN in Y direction) for the P1, P2, and P3 bridge piers, respectively. The corresponding reduced-scaled peak column base shear predicted by the NLRHA in X direction were about 272 kN, 800 kN, and 364 kN (144 kN , 891 kN, and 220 kN in Y direction) for the P1, P2, and P3 specimens, respectively. Two actuators of 980kN at the P2 specimen in both directions should be adequate for the PDTs. Similarly, one actuators of 980kN at P1 or P3 specimens also in both directions should be adequate for the PDTs. Fig. 13 shows the comparison of the maximum bridge column drift distribution under the applications of the 2/50 event obtained from the analytical results. The peak column drifts predicted by NLRHA were about 1.36% (X direction, at P1 specimen) and 1.09% radians (Y direction, at P2 specimen). Fig. 14 shows the analytical peak lateral bridge column top displacements under the applications of 2/50 event (P2 specimen). The peak lateral column top displacements predicted by NLRHA in X direction were about 136 mm (at P1 column), and 136 mm (at P3 column).

Test Results

A total of four PDTs were conducted, which were sequenced as follow: (1) M65R40T4 scaled to represent a 50/50 hazard intensity, i.e., with a 50% chance of exceeding in 50 years, (2) CHY024NS scaled to a 10/50 hazard intensity, which represents the design basis earthquake, (3) M65R40T4 scaled to a 2/50 hazard, and (4) CHY024NS scaled to a 10/50 hazard – identical to loading in (2). Figs. 15 and 16 present the experimental base shear and roof displacement time history in the 2/50 hazard level for P2 column, which is the largest specimen (6-meter column height) located at NCREE. The analytical prediction by PISA3D was also shown in the figures. It was found that all DSCFT columns have good seismic performance during the four tests. Also, that the roof displacements and the base shear simulated by PISA3D as in Figs. 18 and 19 were satisfactory with the test results. There was no column-to-basement connection failure for three specimens, thus, it was confirmed that the proposed DSCFT connection details and design procedures were satisfied to develop the full plastic moment of the composite DSCFT columns.

Conclusions

Based on the test and analytical results, summary and conclusions were made as follows:

1. The peak column base shear predicted by the NLRHA in X direction were about 6812 kN, 5000 kN, and 9112 kN (3590 kN , 5568 kN, and 5501 kN in Y direction) for P1, P2, and P3 bridge piers, respectively. The corresponding reduced-scaled peak column base shear predicted by the NLRHA in X direction were about 272 kN, 800 kN, and 364 kN (144 kN , 891 kN, and 220 kN in Y direction) in the P1, P2, and P3 specimens, respectively.
2. The peak column drifts predicted by NLRHA were about 1.36% (X direction, at P1 specimen) and 1.09% radians (Y direction, at P2 specimen).
3. The peak lateral column's top displacements predicted by NLRHA in X direction were about 136 mm (at P1 column), 136 mm (at P3 column) in both directions.
4. DSCFT bridge pier system performed extremely well after the application of four earthquake load effects.
5. Test results confirmed that the earthquake responses of the DSCFT bridge piers system can be

predicted satisfactorily using both PISA3D and OpenSEES.
6. Tests confirmed that the networked testing architecture implemented for the ISEE is very effective in disseminating real time test results through the internet, especially for large scale experimental tests.

Acknowledgments

The research supports provided by the Natural Sciences and Engineering Research Council Canada and the National Science Council Taiwan are gratefully acknowledged. The authors would also like to acknowledge the technical information and assistance provided by Professor H. A. Khoo of Carleton University, and C. H. Chen and W. C. Cheng of NCREE.

References

American Institute of Steel Construction (AISC), 1994. Manual of steel construction: Load and resistance factor design (LRFD), 2nd Ed., Chicago.

AISC (American Institute of Steel Construction), 1994. Seismic Provisions for Structural Steel Buildings, Chicago, IL.

Barker R.M. and Puckett J.A., 1997. Design of Highway Bridges. New York: John Wiley.

Demetrios E.T., 1995. Bridge Engineering: Design, Rehabilitation, and Maintenance of Modern Highway Bridges, New York: McGraw Hill.

DOT, 1995. “Highway Bridge Seismic Provision and Commentary”, Taipei.

Filippou, F. C., 1996. FEDEAS: Nonlinear Static Dynamic Analysis from Research to Practice. Proceedings, ASCE Structures Congress, Chicago, USA.

Harris, H. G. and Sabnis, G. M., 1999. Structural Modeling and Experimental Techniques (2nd ed), Boca Raton: CRC Press.

Hsu H.L. and Lin J.L., 1997. Inelastic Behavior of Sandwich Box Column under Combined Loading. Proceedings of 6th U.S. National Conference on Earthquake Engineering.

ICC, 2000. Internal Building Code, Whittier, CA.

Kim, J. K., 2004. KOCED Collaboratory Program. Proceedings of the 2004 ANCER Annual Meeting: Networking of Young Earthquake Engineering Researchers and Professionals, Hawaii, USA.

Lin Y.S., 2001. Cyclic Response of Double-Skin Concrete Filled Steel Tube Column-to-Foundation Connections, Master thesis, Department of Civil Engineering, National Taiwan University, Taipei, Taiwan (in Chinese).

McKenna, F. and Fenves, G. L., 2000. An Object-Oriented Software Design for Parallel Structural Analysis. Proceedings of Advanced Technology in Structural Engineering, Structures Congress 2000, ASCE, May 2000.

NBC, 2005. National Building Code 2005 Draft. Canadian Commission on Building and Fire Codes, Canada.

Reitherman, R., 2004. A Short History and Overview of NEES, A Short report, available at homepage of NEES Consortium Inc. Homepage web site: http://www.ness.org/.

Shome, N., C. A. Cornell, P. Bazzurro, and J. E. Carballo, 1998. Earthquake, records, and nonlinear responses, Earthquake Spectra, 14(3), 469-497.

Tsai, K.C. and B. Z. Lin, 2003. User Manual for the Platform and Visualization of Inelastic Structural Analysis of 3D Systems PISA3D and VISA3D, Report No. CEER/R92-04, Center for Earthquake Engineering Research, National Taiwan University, Taipei.

Tsai, K.C., Lin, M.L., Lin, Y.S. and Wei, S.S., 2005. Nonlinear Responses of Double-Skin Concrete Filled Steel Tube Bridge Pier-to-Foundation Joints. Journal of Earthquake Engineering and Engineering Seismology” (submitted).

Wang, K. J., Wang, S. J., Yang, Y. S., Cheng, W. C., and Tsai, K. C., 2003. ISEE: Internet-Based Simulations for Earthquake Engineering Part II: The Application Protocol Approach. Proceedings

of the International Workshop on Steel and Concrete Composite Construction, Taiwan, 311-320.

Wei, S. S., 2002. Cyclic responses of embedded double-shin concrete filled steel tube column-to-foundation connections, *Master Thesis*, Department of Civil Engineering, National Taiwan University, Taipei, Taiwan (in Chinese).

Yang, Y. S., Wang, S. J., Wang, K. J., Tsai, K. C., and Hsieh, S. H., 2003. "ISEE: Internet-Based Simulations for Earthquake Engineering Part I: The Database Approach." Proceedings of the International Workshop on Steel and Concrete Composite Construction, Taiwan, 301-310.

Zhong, S.T., 1999. Concrete Filled Steel Tubular Structures, Heilengjiang, China.

Figures and Tables

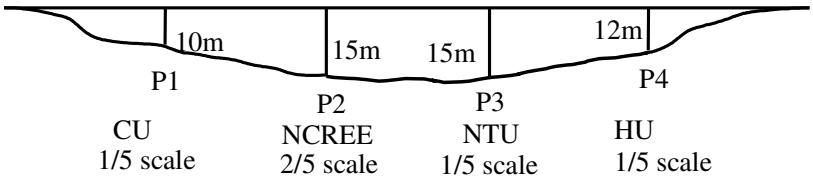

Figure 1. Elevation of the multi-span bridge system in the experiment.

Table 1. Vancouver design spectral acceleration for 2%/50 year probability (NBC, 2005).

Sa(0.1)	Sa(0.15)	Sa(0.2)	Sa(0.3)	Sa(0.4)	Sa(0.5)	Sa(1.0)	Sa(2.0)	PGA
0.80	0.95	0.96	0.84	0.74	0.66	0.34	0.18	0.47

unit: g

Table 2. Stiffness and strength of the superstructure and piers.

	Superstructure	Piers			
		P1	P2	P3	P4
EI (MN-m2)	65340.0 (strong-axis)	23492.2	50920.9	23492.2	50920.9
EA (MN)	414520	92566.1	137228.1	92566.1	137228.1
J (m4)	5.96	0.115	0.243	0.115	0.243
Em (MPa)	N.A.	409947.1	397187.1	409947.1	397187.1
Fmy (MPa)	248.2	741.7	711.7	741.7	711.7

Table 3. Sectional properties of the prototype bridge.

Pier No.	P1	P2	P3	P4
I_{SE} (m^4)	0.12	0.26	0.12	0.26
I_{SI} (m^4)	0.02	0.04	0.02	0.04
$I_S = I_{SE} + I_{SI}$ (m^4)	0.14	0.30	0.14	0.30
I_C (m^4)	1.81	3.74	1.81	3.74
J_C (m^4)	3.62	7.49	3.62	7.49
J_{SE} (m^4)	0.24	0.52	0.24	0.52
J_{SI} (m^4)	0.04	0.09	0.04	0.09
A_C (m^2)	4.77	6.86	4.77	6.86
A_{SE} (m^2)	0.16	0.23	0.16	0.23
A_{SI} (m^2)	0.07	0.11	0.07	0.11
$A_S = A_{SE} + A_{SI}$ (m^2)	0.23	0.34	0.23	0.34
A_{SVE} (m^2)	0.079	0.12	0.079	0.12
A_{SVI} (m^2)	0.036	0.06	0.036	0.06
$J = J_C + J_{SE} + J_{SI}$ (m^4)	3.903	8.09	3.903	8.09
α	0.047	0.05	0.047	0.05

Table 4. Details of full-scale DSCFT bridge piers.

Piers	P1	P2	P3	P4
Column height	10 m	15 m	15 m	12 m
Axial Load(kN)	10200	10420	10410	10940
Lateral force requirement(kN)	2.55E+03	2.18E+03	2.12E+03	2.80E+03
Moment requirement(kN-m)	25520	32730	31860	33600
Diameter of external tube	2.5 m	3.0 m	3.0 m	3.0 m
Diameter of internal tube	1.5 m	1.8 m	1.8 m	1.8 m
Thickness of external tube	2cm	2.5cm	2.5cm	2.5cm
Thickness of internal tube	1.5cm	2cm	2cm	2cm
Axial load capacity P0(kN)	116854	170912	170912	170912
Moment capacity (kN-m)	57599	95277	57685	95277
Aspect ratio of axial load (%)	8.74%	6%	6%	6.4%
Aspect ratio of moment (%)	44.31%	34.35%	55.23%	35.27%

Table 5. Details of scaling-down specimens.

Pier	P1(CU)	P2(NCREE)	P3(NTU)
Scaling factor	20%	40%	20%
Column height	2 m	6 m	3 m
Diameter of external tube	0.5 m	1.2 m	0.6 m
Diameter of internal tube	0.3 m	0.72 m	0.36 m
Thickness of external tube	0.4cm	1cm	0.5cm
Thickness of internal tube	0.3cm	0.8cm	0.4cm
Axial load capacity P0(kN)	4674	27346	6836
Aspect ratio of axial load(%)	8.74%	6%	6%
Applied Axial Load(kN)	408	1667	416
Moment capacity(kN-m)	452	6589	823

Table 6. Design details of DSCFT-to-foundation connections.

Spec.	h (m)	h_e (m)	$\frac{h_e}{D}$	M_{base} (kN-m)	$M_{bearing}$	$M_{overhang}$	M_{bolt}	$\frac{M_{bearing}}{M_{base}}$	$\frac{M_{overhang}}{M_{base}}$	$\frac{M_{bolt}}{M_{base}}$	Amount of bolts	Strength Ratio
P1(CU)	1.0	0.5	1.0	511	591	151	340	1.16	0.30	0.67	10-A325 M16	2.13
P2 (NCREE)	1.72	0.96	0.8	7644	5070	1008	5243	0.66	0.13	0.69	10-A325 M16	1.48
P3(NTU)	1.0	0.5	0.83	961	684	296	454	0.71	0.31	0.47	24-A325 M32	1.49

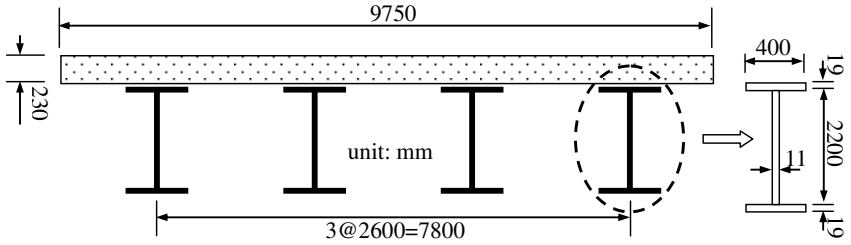

Figure 2. Sizes of superstructure.

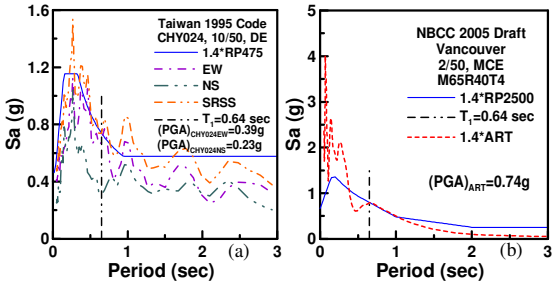

Figure 3. Design acceleration spectra (a)10/50 (b)2/50 hazard levels.

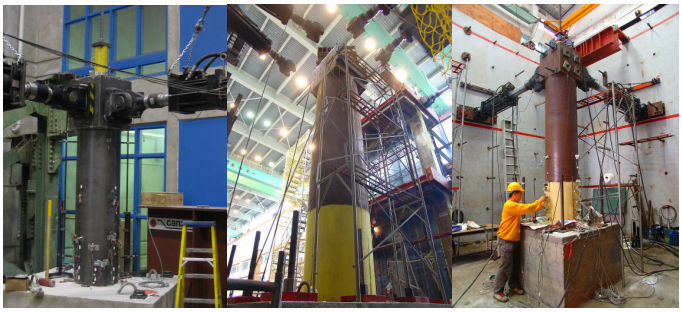

(a) P1, at CU (b) P2, at NCREE (c) P3, at NTU

Figure 4. Experimental set-up.

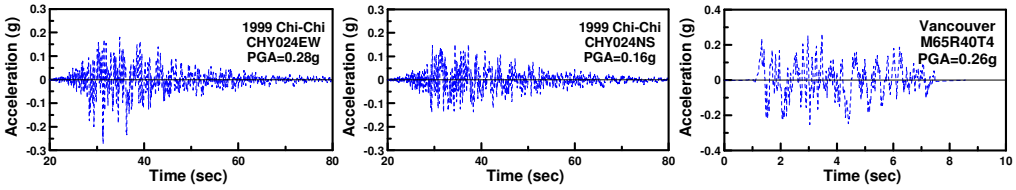

Figure 5. Original ground accelerations used in test (before scaling).

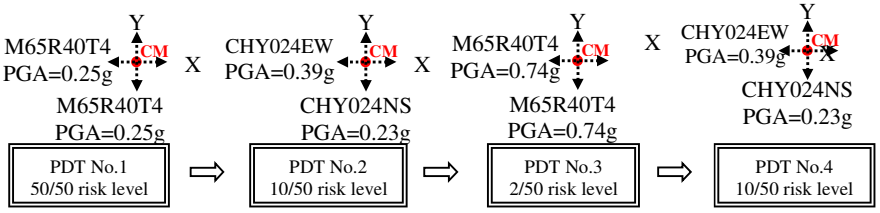

Figure 6. Earthquake scenario for the PDTs of DSCFT bridge pier system.

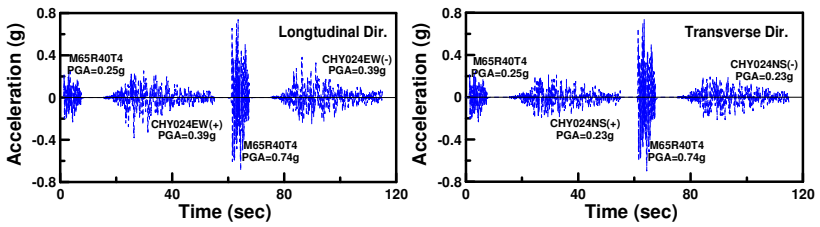

Figure 7. Earthquake sequences for the PDTs.

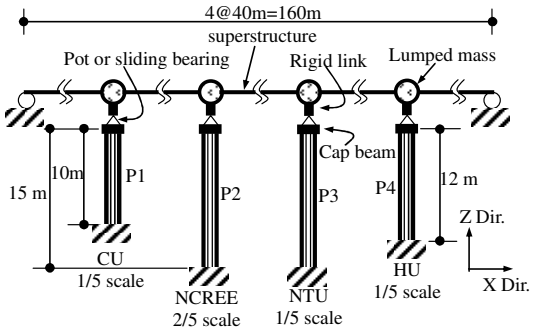

Figure 8. Structural model for the prototype bridge system.

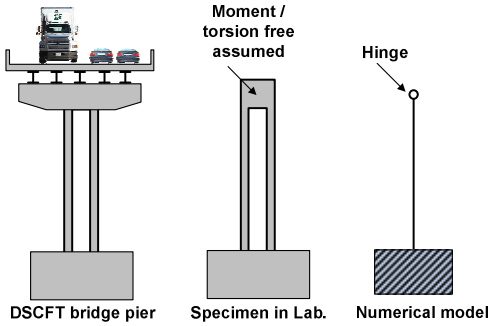

Figure 9. Simplified DSCFT Bridge pier for specimen and numerical analysis.

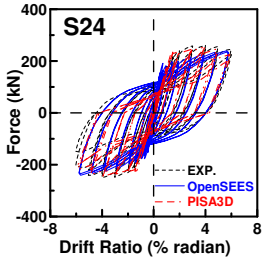

Figure 10. Force-Disp. curves of DSCFT columns.

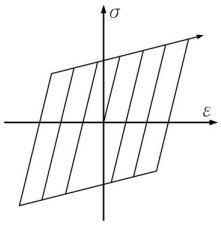

Figure 11. Bilinear element model.

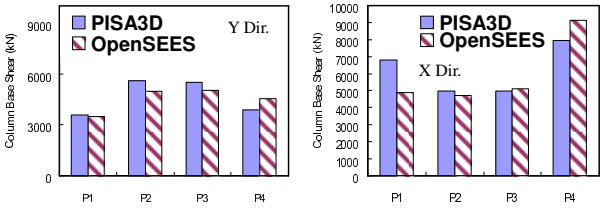

Figure 12. Peak bridge column base shear (2/50 hazard levels).

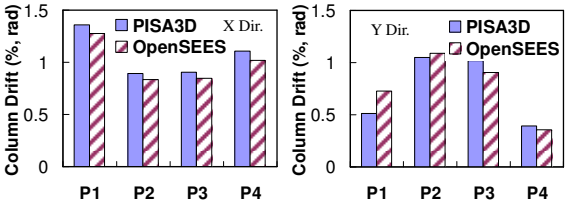

Figure 13. Peak bridge column drift (2/50 hazard levels).

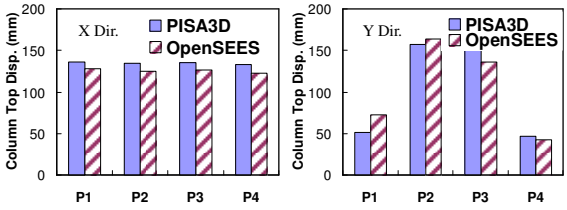

Figure 14. Peak bridge column top displacement (2/50 hazard levels).

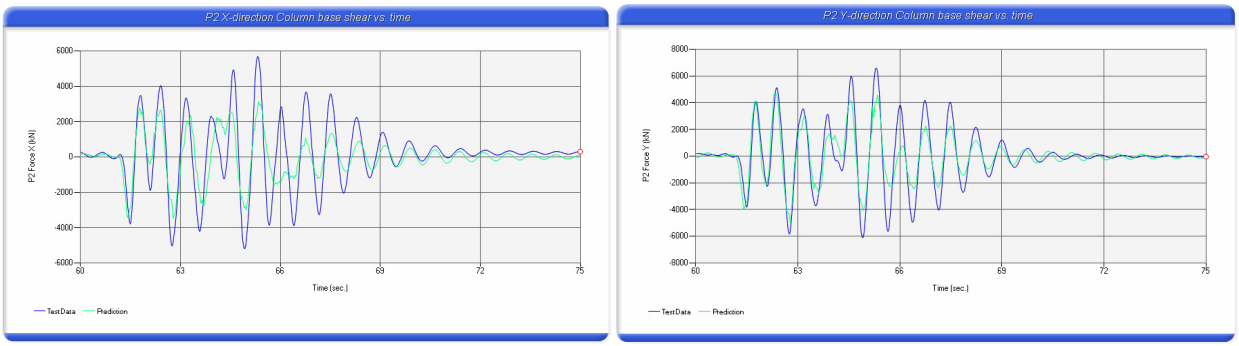

Figure 15. P2 column (NCREE) base shear history (2/50 hazard levels).

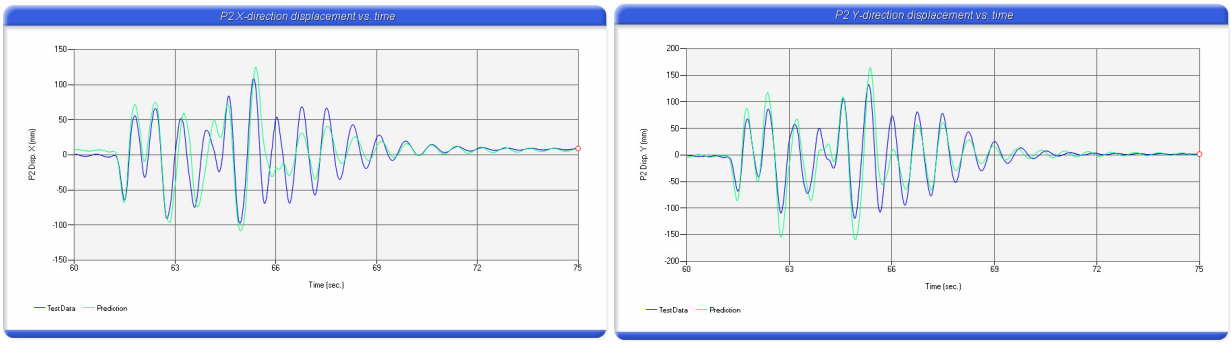

Figure 16. P2 column (NCREE) displacement history (2/50 hazard levels).